Author: Gagestein, B.
Title: Chemical tools to study lipid signaling
Issue Date: 2020-12-16

Chapter 2

Lipid photoaffinity probes[1]

Introduction

Photoactivatable lipids are synthetic analogues of natural lipids that are designed to retain the overall structure and interactions of the parent lipid, and contain a photoactivatable moiety that can form an irreversible covalent bond with its protein interacting partner upon irradiation. This covalent bond essentially 'freezes' the interaction and allows for investigation of lipid-protein interactions as they occur in their complex native environments.[2]

To generate a photoaffinity probe, a number of photoreactive moieties are available with differing synthetic accessibility, reactivity, efficiency and structural impact. Three photoreactive groups are routinely used: diazirines, benzophenones and aryl azides (Table 1). The reactivity of the highly energetic intermediates formed upon irradiation affects their labeling properties. The reactive carbene formed upon irradiation of a diazirine reacts for a significant portion with water or intramolecularly, reducing its labeling efficiency. However, its reactivity ensures a short half-life, allowing less time for the probe to diffuse and react nonspecifically (that is, with proteins other than its natural interaction partner).[3] Nonetheless, some of the excited diazirine isomerizes to the linear diazo form, which has a longer lifetime and is less reactive. Irradiation of a benzophenone results in the formation of a less reactive diradical, which has more time to diffuse and to react nonspecifically.[4] However, it favors the insertion into C-H bonds as reaction with water results in a reversible hydrate, thereby yielding higher labeling efficiencies.[5]

Irradiation of an aryl azide leads to the formation of a nitrene, which has a high reactivity, but like the diazirine, suffers from spontaneous rearrangement reactions resulting in other reactive species with a longer lifetime.[6] Another drawback of the aryl azide is that the wavelength required to activate an aryl azide is damaging to biological material.

Table 1 | Structures and properties of most commonly used photoactivatable groups.[5,7,8]

Structure	Most reactive intermediate	Absorption	Reactivity	Remarks
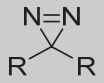 Diazirine	 Carbene	Activated at 350-360 nm	High, lifetime 21 ns	Can isomerize to less reactive diazo form
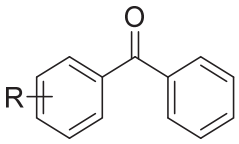 Benzophenone	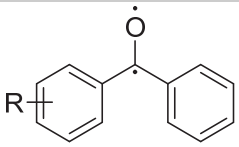 Diradical	Activated at 350-360 nm	Slow, lifetime 80-120 µs	Diradical can collapse to reform the benzophenone
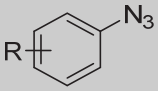 Aryl azide	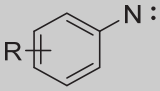 Nitrene	Activated at 254 nm	Medium to high	Can rearrange to form less reactive intermediates

The choice of photoactivatable group depends on a number of factors. Since their conception, lipid probes have seen a shift from benzophenones to diazirines. Contributing factors to this trend have been increased synthesis abilities, the desire for smaller modifications and the application in a relatively water-free inner membrane, where the reactivity of the diazirine is optimal. In this chapter, lipid photoaffinity probes for glycero(phospho)lipids, fatty acyls, sphingolipids and sterols reported in the last decade and their main discoveries are discussed.

Lipid-based photoaffinity probes

Glycero(phospho)lipids

One of the most well-studied lipid classes is the family of glycero(phospho)lipids. Their amphipathic nature is essential for the formation of lipid bilayers and they are universally present in cellular membranes. Glycerolipids are composed of a glycerol backbone that has been mono-, di- or trisubstituted with a fatty acyl group. In glycerophospholipids, the *sn*-3-position is esterified with a phosphate moiety, which in turn can be substituted with different head groups. The most common substituents are a choline, ethanolamine, glycerol, serine or inositol, thereby giving rise to various classes of glycerophospholipids, such as phosphatidylcholine (PC), phosphatidylethanolamine (PE), phosphatidylglycerol (PG), phosphatidylserine (PS) and phosphatidylinositol (PI), respectively. The length and degree of unsaturation of the fatty acyl groups at the *sn*-1 and *sn*-2 position determine the physical

properties of the glycerophospholipid and its substitution pattern on the phosphate group dictates its protein interactions partners on the membrane surface.[9]

The composition of the different types of lipids and their compartmentalization between cellular substructures does not only determine the physical properties of the biomembrane, but also regulates protein activity, localization and cellular signaling events via lipid-protein interactions. Such types of interactions can be discovered via application of lipid-based photoaffinity probes. Phosphatidylserine lipids, for example, are primarily found on intracellular membrane surfaces. When this asymmetry is disturbed during apoptosis, PS presentation is a trigger for phagocytosis. PS analogues **1-5** (Figure 1), containing a benzophenone and alkyne click handle were developed, and shown to label interacting proteins, such as prothrombin-1.[10]

Phosphatidylcholine-based probes were made to study membrane-associated proteins, which are traditionally underrepresented in proteomic experiments.[11] The goal was to detect proteins interacting with the phospholipid head groups of inner mitochondrial membranes. To this end, a photoreactive group was installed on the solvent-exposed head group of the lipid. Aryl azide probe **6** and benzophenone probe **7** (Figure 1) were used to isolate proteins from *Saccharomyces cerevisiae* mitochondria. The identified targets consisted of known membrane-interacting proteins, including Gut2p and Cox2p, but also new proteins not previously known to be membrane-associated, such as Ald4p and Mrp7p. Of note, the authors concluded that aryl azide **6** is the preferred probe due to lower background labeling compared to benzophenone **7**.[11]

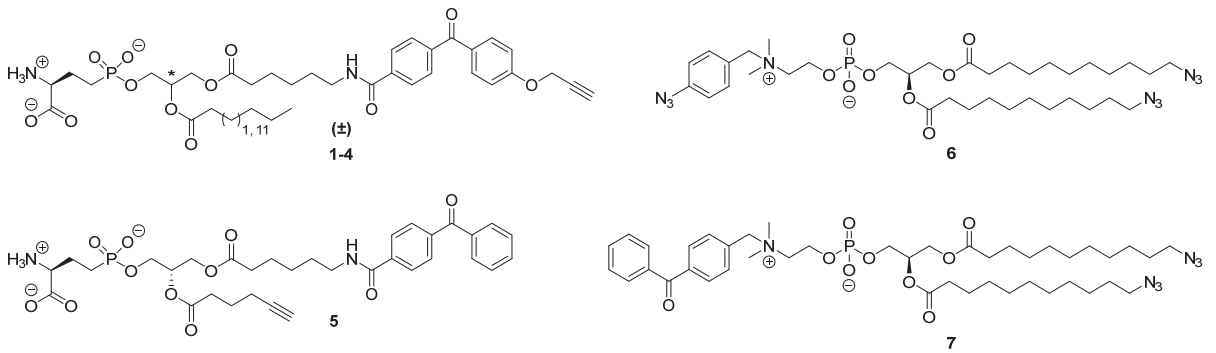

Figure 1 | Structures of photoaffinity probes based on phosphatidylserine **1-5** and phosphatidylcholine **6-7**.

Phosphatidylinositol polyphosphates are a family of signaling lipids that act as anchors for protein association to the membrane. To discover interacting proteins, two probes based on phosphatidylinositol 3,4,5-triphosphate were synthesized.[12] Probes **8** and **9** (Figure 2) were tested on the purified pleckstrin homology domain of protein kinase B, a known phosphatidylinositol phosphate binder. Probe **8** gave better signal, which was attributed to its shorter linker length, which positioned the benzophenone closer to the protein. Probe **8** was also applied to MDA-MB-435 cell extracts, which resulted in the identification of 265 phosphatidylinositol 3,4,5-triphosphate-binding proteins.[12] To study the membrane-binding domain of PON1, a high-density lipoprotein (HDL)-associated protein, phospholipid probe **10** was made (Figure 2). Covalent photocrosslinking of **10**, digestion and mass spectrometry analysis resulted in the identification of several closely localized residues on the surface of PON1, revealing the HDL-binding domain.[13]

To study the ability of cardiolipin to form a complex with the mitochondrial protein cytochrome *c*, photoaffinity probes **11-13** were synthesized (Figure 2).[14] These probes all induced similar or higher cytochrome *c* peroxidase activity compared to endogenous tetraoleoyl cardiolipin. This indicated that the central hydroxyl group is not necessary for activation. No follow-up study applying the labeling functionality has appeared yet.[14]

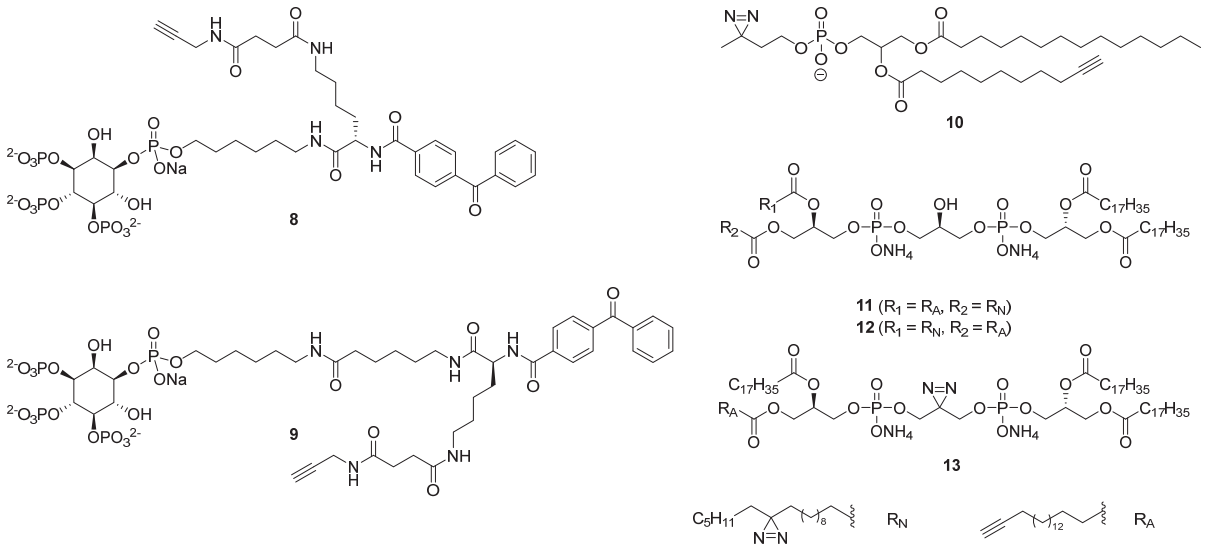

Figure 2 | Structures of photoaffinity probes based on phosphatidylinositol 3,4,5-triphosphate **8-9**, phospholipid **10** and cardiolipin **11-13**.

Currently, several photoactivatable analogs of phosphatidylcholines are commercially available. It is argued, however, that lipids supplied to a cell are distributed differently than endogenously produced lipids, which are synthesized within the cell. This may distort the interaction profile reported by the probe.[15] Moreover, palmitoyl- and myristoyl-based probes can be incorporated in various glycerolipids or as post-translational modifications (PTMs), thereby further complicating the analysis of a photoaffinity experiment. To solve these issues, Yao and co-workers reported on alkyne-containing choline **14** and diazirine-containing fatty acid **15** (Figure 3).[16] When cells were incubated with these separate probe components, the subsequent photoaffinity experiment only captured the proteins that interact with the *in situ* synthesized phosphatidylcholine probe (**14**+**15**). This strategy yielded an interaction map of 211 high-confidence PC-interacting proteins, mostly present in the cytosol, endoplasmic reticulum (ER), mitochondria and nucleus. The authors concluded that the double incorporation strategy offered improvement for global mapping of genuine protein-lipid interactions and indicated that the strategy is expandable to different lipid classes, such as phosphatidylinositols.[16]

Monogalactosyldiacylglycerol (MGDG) is a type of anti-inflammatory signaling lipid.[17] Three photoactivatable probes (**16-18**) were synthesized to elucidate its mode of action (Figure 3). The linolenoyl groups were replaced with a similar photoaffinity-click fatty acid (pacFA) or a minimalist linker[18] was added to the sugar moiety. When tested in an inflammatory assay, **16** did not show any activity, while **17** and **18** had comparable activity to MGDG. This indicated that an unmodified galactosyl moiety is essential for MGDG activity. Moreover, when incubated, UV-exposed and washed, **17** lost all anti-inflammatory activity whereas **18** was still active. This implied that **18** was capable of both binding and labeling unidentified targets without disrupting its biological function. With structure **16** as negative control, TLR-4 was identified as a probe target in human chondrocytes. Subsequent orthogonal experiments demonstrated MGDG acted as TLR-4 antagonist.[19]

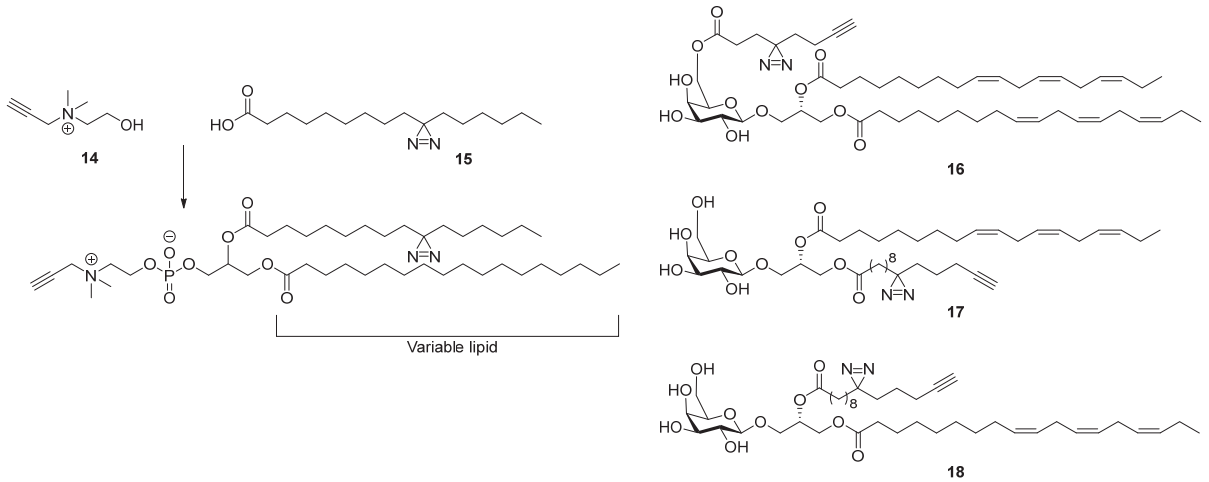

Figure 3 | Structures of photoaffinity probes based on phosphatidylcholine **14**+**15** and dilinolenoyl MGDG **16-18**.

Recently, caged photoaffinity probes based on diacylglycerol (DAG) (**19**, Figure 4), saturated fatty acid (**20**, Figure 5), and sphingosine (**21**, Figure 6) were developed by Schultz and co-workers.[20] These probes were used to study biologically active signaling molecules with temporal, spatial, and subcellular resolution. The caging groups consists of a fluorescent coumarin group, which prevents recognition of the lipid by the cellular machinery. This caging group can then be released upon irradiation with a wavelength that does not activate the diazirine moiety. Microscopy experiments indicated that all probes were indiscriminately localized to internal membranes and the cytoplasm. Uncaging, photocrosslinking and ligation with a fluorophore showed that each probe localized to distinct cellular components. It also proved feasible to use the uncaging for controlled release of DAG. Elevated DAG levels are known to trigger translocation of C1-domain-containing proteins to the plasma membrane.[21] When **19** was uncaged in HeLa cells, immediate translocation of C1-linked green fluorescent protein (GFP) was observed.[20] Moreover, DAG turnover could be quantified on a population-wide and single-cell level. The authors suggested that standard biochemical experiments to measure DAG metabolism are inherently flawed, since they only measure combined lipid transport and metabolism. Moreover, striking differences were found between DAG turnover on a cell-to-cell level, indicating that heterogeneity might be an underrated complication of lipid signaling.[20] In addition, a pulldown experiment with probes **19-21** was performed using HeLa cell proteome affording 130 **19**-specifically binding proteins. As the probe contains arachidonic acid, the hits were compared to the targets of arachidonic acid-based probes **22** and **23** (Figure 5). Remarkably, only 17 of the proteins identified using DAG probe **19** were previously identified with probes **22** and **23**, showing that probe **19** has mostly genuine DAG-specific interactions. Overall, the two activatable functionalities within the probe allowed to investigate different aspects of the lipids such as the protein interaction partners, metabolism and signaling functions.[20]

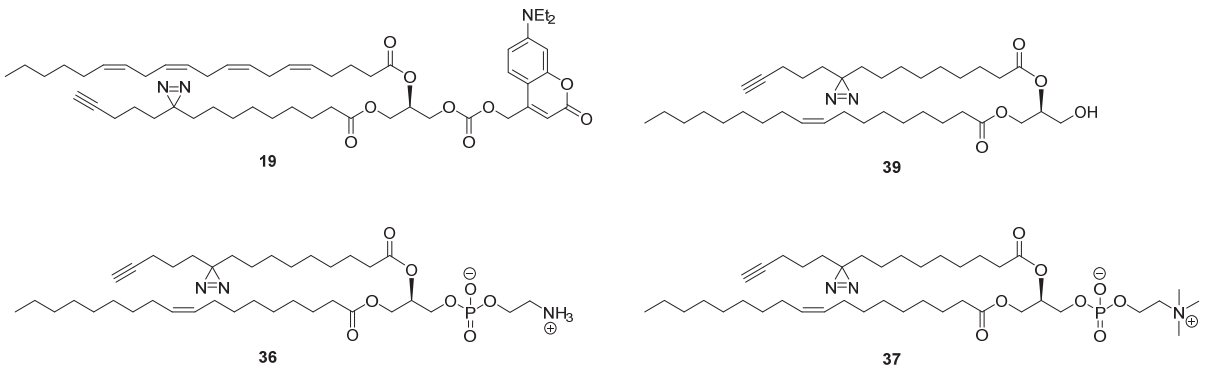

Figure 4 | Structures of photoaffinity probes based on diacylglycerol **19** and **39**, phosphatidylethanolamide **36** and phosphatidylcholine **37**.

Fatty acids and their derivatives

Fatty acids are constituents of other lipid classes, such as glycerol(phospho)lipids, glycolipids and ceramides, but they also have their own signaling roles. In addition, they can be incorporated in proteins as post-translational modification (PTM), thereby anchoring the protein to the membrane. Furthermore, oxidative enzymes, such as lipoxygenases, cyclooxygenases and cytochrome P450s metabolize polyunsaturated fatty acids into bioactive signaling molecules. For example, endothelium-derived epoxyeicosatrienoic acids (EETs) are lipid signaling molecules with various biological activities.[22] In search of a high-affinity G protein-coupled EET receptor for 14,15-epoxyeicosatrienoic acid, epoxide-containing lipid **24** equipped with a photoactivatable aryl azide and radioactive iodide as reporter group was synthesized (Figure 5). The probe showed EET agonist activity and labeled a 47 kDa band which could be outcompeted with several EET agonists and antagonists.[23] However, with no bioorthogonal ligation handle present, the protein could not be identified.

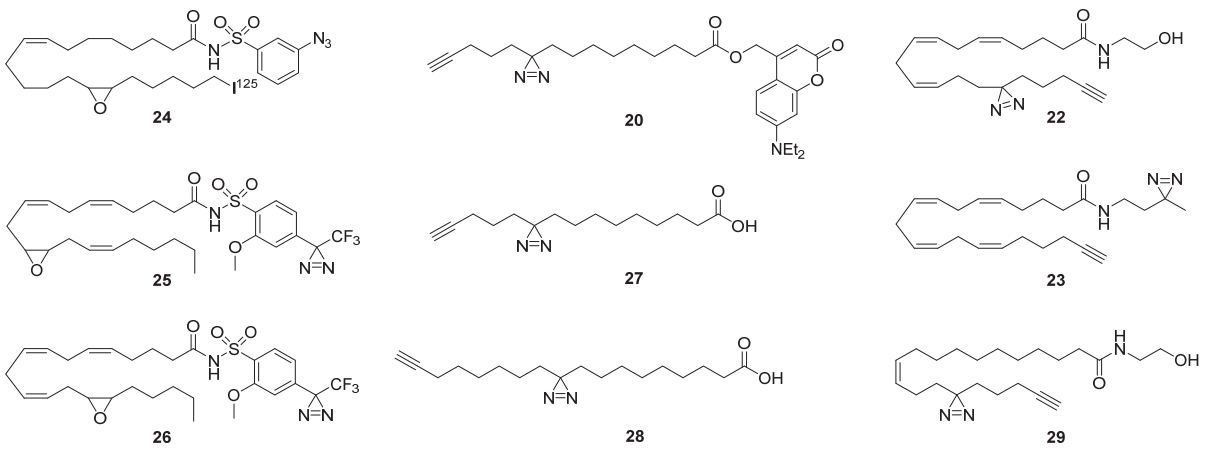

Figure 5 | Structures of photoaffinity probes based on 14,15-epoxyeicosatrienoic acid **24-26**, bifunctional lipid probes **27-28**, trifunctional lipid probe **20**, anandamide-based probes **22**, **23** and probe **29**.

The structurally related probes **25** and **26** (Figure 5) have been used to study the binding mode of EETs in the soluble epoxide hydrolase (sEH) enzyme.[24] Photoaffinity experiments combined with computational modeling indicated that the stereochemistry of the epoxide dictates the binding orientation of the substrate into the enzyme.

Bifunctional probe **27** (Figure 5) was synthesized to study *in vivo* protein-lipid interactions.[2] Fatty acids can be incorporated in different lipid classes and in proteins as PTM. Proteomic analysis using **27** resulted in the identification of a large number of lipid-interacting proteins in CHO and HeLa cells. Enrichment of proteins by UV irradiation indicated noncovalent interactions, while proteins that were enriched in the absence of UV irradiation were designated as putative palmitoylated proteins. This observation was supported by an increase in identified palmitoylated proteins when the incubation time was increased. The authors continued by demonstrating the usage of the probe to visualize lipid-interacting proteins in

nematode larvae using fluorescence microscopy. Overall, this report demonstrates the versatility of bifunctional probes in studying protein-lipid interactions.[2]

Other groups have also exploited metabolic incorporation of lipids as PTM. For example, probe **28** (Figure 5) was incorporated in S-palmitoylated membrane proteins.[25] The photoaffinity group allowed the capture of protein-protein interactions of interferon-induced transmembrane protein 3 (IFITM3), a protein with antiviral properties. This method was validated by studying VAPA–a known interaction partner of IFITM3–after which a pulldown experiment afforded 12 novel interaction partners of IFITM3.[25]

Anandamide is a signaling lipid involved in neurotransmission. To map anandamide-binding proteins, photoaffinity probes **22** and **23** were synthesized in the lab of Cravatt. More than a thousand interacting proteins were identified in Neuro-2a and HEK-293 cells, including NUCB1, NENF and VAT1. Probes **22** and **23** were subsequently employed to discover ligands for the lipid-binding pockets of said targets using competitive fluorescence polarization assays.[26] In addition, lipid probes **22**, **23** and oleoylethanolamide-based **29** (Figure 5) were utilized in another study to determine the selectivity profile of small molecules occupying lipid-binding pockets. This strategy was referred to as lipid-protein interaction profiling (LiPIP).[27]

Sphingolipids

Sphingolipids are lipids that have sphingosine or a sphingosine derivative as a scaffold. Similar to glycerolipids, most of the sphingolipids exist in the form of a phosphate ester and have a fatty acyl attached through an amide bond. Sphingomyelin, one of the most common sphingolipids, serves mainly a structural purpose, but its derivatives are increasingly recognized as important signaling molecules.

The last decade has witnessed a continuous progression in the development of chemical probes to identify sphingolipid-binding proteins. For example, Haberkant *et al.* have synthesized tritium-functionalized probes **30** and **31** (Figure 6), which are rapidly incorporated into sphingolipids when applied to tissue cultures.[28] Caveolin-1 and nicastrin were identified as sphingolipid-interacting proteins. In 2010, photoactivatable sphingosine **32** (Figure 6) was made and co-incubated with radioactive [^{3}H]choline in fibroblasts from healthy subjects or patients with Niemann-Pick A disease.[29] The sphingomyelin storage was found to be dysregulated in fibroblasts of the patients.

In 2015, Schultz and co-workers developed photoaffinity-click sphingosine (pacSph) **33** (Figure 6), which was used to identify 186 pacSph-interacting proteins.[30] As a control, fatty acid probe **27** was used. Although probes **27** and **33** are based on different lipids and are metabolized via different pathways, substantial overlap between the interacting proteins was found. Four potential issues were mentioned: (i) both lipid probes could be incorporated into

phosphatidyl choline lipids, (ii) proteins may have two or more lipid-binding sites, (iii) a single lipid-binding site may be able to recognize multiple lipids, and (iv) alterations made on the lipids may alter their physiochemical properties.[30] Nevertheless, pacSph probe **33** proved to be a more versatile tool to discover new sphingosine-binding proteins compared to **30** and **31**. The probe was further developed into trifunctional pacSph **21**, which was used in similar experiments to afford 64 pacSph-specific binding proteins after uncaging,[20] of which only 14 were also found using non-caged pacSph **33**.

Since pacSph **33** has become commercially available, other groups have also employed it in their research of sphingolipids. PacSph **33** was used to distinguish between sphingolipid-protein interactions resulting from ceramides synthesized through ceramide synthase 5 (CerS5) or CerS6. This resulted in the discovery that only CerS6-derived sphingolipids bind to the mitochondrial fission factor (Mff).[31] In another study, pacSph **33** was used to visualize the localization of pacSph by microscopy and its binding to the SPCA1 calcium pump in gel-based experiments.[32]

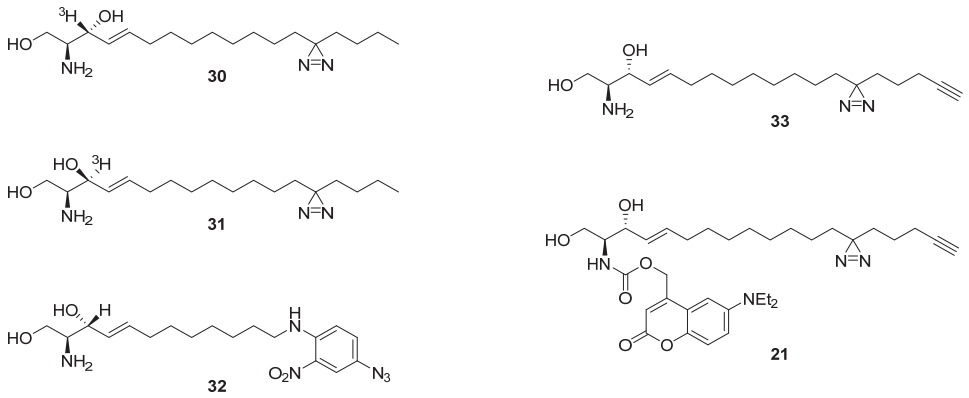

Figure 6 | Structures of photoaffinity probes based on sphingosine **30**, **31**, **32**, **33** and **21**.

Ceramide, a sphingosine containing a fatty acyl amide, is a signaling molecule with pro-apoptotic activity. In search of ceramide-binding proteins, photoaffinity probes **34-39** (Figures 4, 7) with pacFA **27** as basis were developed by Holthuis and co-workers.[33] The targets of ceramide probe (pacCer) **34** were compared to the interaction partners of glucosylceramide (pacGlcCer) **35** in cytosolic fractions of various cell lines. A protein with a StAR-related lipid-transfer domain, CERT, was chosen as model protein to study structure-activity relationships of the lipid-binding pocket. This was done using probes **34-39** to distinguish probe-specific interactions (Figures 4, 7).[33] This set of probes was used by the same group to study ceramide binding to VDAC2, which was found to be a direct effector of ceramide-mediated cell death.[34] Since it has become commercially available, other groups have used pacCer **34** to study its binding to tubulin[35] and downstream effect on VDAC1 closure in mitochondria.[36]

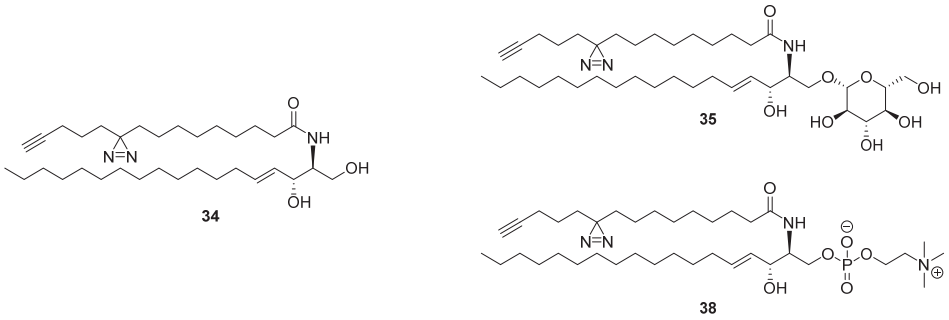

Figure 7 | Structures of photoaffinity probes based on ceramide **34**, glucosylceramide **35** and sphingomyelin **38**.

Sterols

Sterols are lipids with rigid, fused rings with one or more hydroxyl groups, which gives them amphiphilic properties. Cholesterol is the most abundant sterol found in mammalian cells. Cholesterol alters the fluidity of the membrane and is a constituent of lipid rafts, which are liquid-ordered regions of the plasma membrane high in cholesterol and glycosphingolipids, sequestering specific proteins.[37] The lipid environment alters the biological properties of the embedded proteins. The noncovalent interaction of sterols to proteins, specifically in lipid rafts, has received a surge of interest in recent years.

Various types of cholesterol-based probes have been synthesized (Figure 8). Structures **40-42** are diastereomers which showed similar protein labeling patterns on gel with the most intense labeling by the trans-sterol structure **40**.[38] In a large-scale proteomics experiment in cells using probe **40**, about 850 proteins were found to be UV-enriched. Nearly 700 of these proteins showed preference over a palmitoylethanolamide-based probe and could be annotated as cholesterol-interacting proteins.

Compounds **43** and **44** were synthesized to map cholesterol binding sites in VDAC1 (Figure 8). Purified recombinantly expressed mouse VDAC1 was used in a top-down and bottom-up proteomics analysis to map the binding pocket. The binding site was found to include Thr83 and Glu73.[39] To study the transfer of cholesterol between NPC1 and NPC2, the linked cholesterol pair **45** has been synthesized to stabilize the protein transition state during the hand-off (Figure 8). Supported by previous studies, the probe was thought to stabilize protein dimer complexes, but no follow-up report has appeared yet.[40]

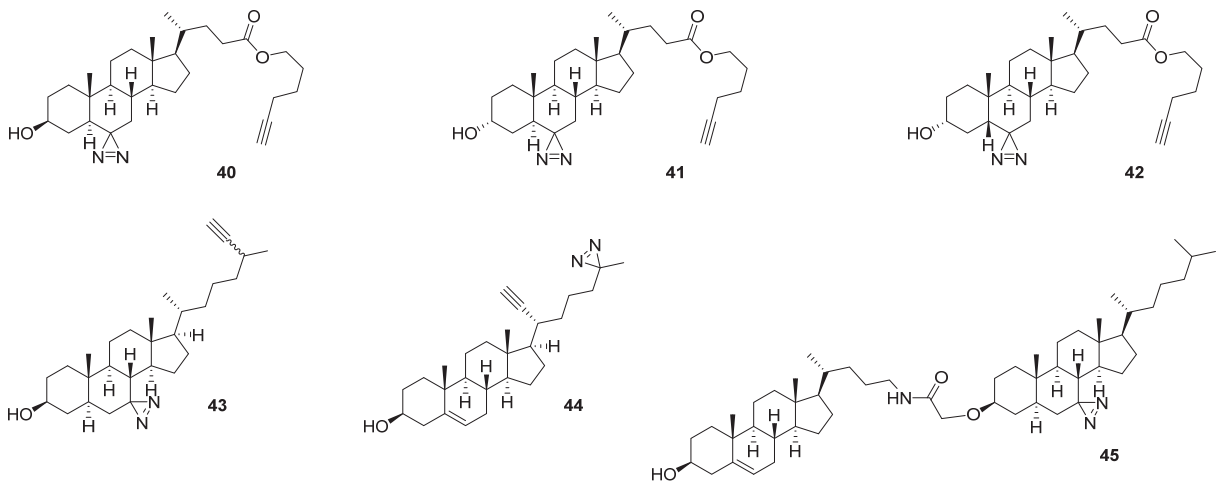

Figure 8 | Structures of photoaffinity probes based on cholesterol **40-45**.

Bile acids are sterols that aid in digestion of dietary lipids, but may also act as signaling molecules regulating lipid and glucose metabolism.[41] Three probes based on bile acids have been synthesized with the diazirine and alkyne located on different parts of the sterol.[42] Probes **46-48** (Figure 9) afforded 331 proteins that were labeled by all three structures and out-competed with a twofold excess of competitor. Three known and three unknown bile acid binding proteins were validated by overexpression, labeling with or without a competitor and immunoblotting. Of note, 146 of these probe targets were shared by cholesterol probe **40**.[38,42]

The development of betulinic acid-based probes, including photoactivatable probes **49** and **50** (Figure 9), has been reported.[43] Probe **49** was armed with a 2-aryl-5-carboxytetrazole, a recently developed photoactivatable linker with high crosslinking efficiency.[44] A pulldown experiment performed with both probes afforded 150 probe targets, which were subsequently triaged using control experiments. This afforded 9 and 13 unique proteins identified by structure **49** and **50**, respectively. Surprisingly, there was no overlap in protein targets between the two probes, which was rationalized by the difference in location and reactivity of the photoactivatable groups.

To explore the molecular mechanisms of oleanolic acid, two probes based on this sterol have been synthesized.[45] To test functional similarity to the parent structure, they were tested in a RMGPa inhibition assay, where **51** showed a twofold and **52** (Figure 9) a fivefold reduction of potency compared to oleanolic acid. Probe **51** labeled two gel bands UV-dependently in soluble proteomes prepared from HepG2 cells which could be outcompeted with oleanolic acid, but the probe targets were not identified.[45]

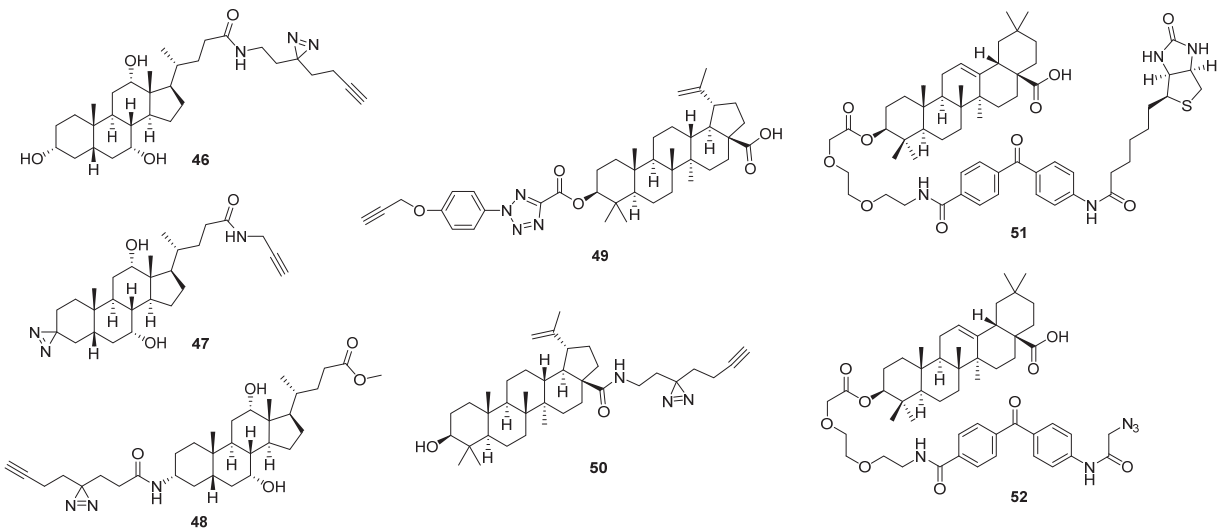

Figure 9 | Structures of photoaffinity probes based on bile acid **46-48**, betulinic acid **49-50** and on oleanolic acid **51-52**.

Promiscuous lipid binding proteins

Chemical proteomic datasets contain a large amount of data with a significant amount of noise, making it challenging to distinguish the specific interaction partners of a probe in a pulldown experiment. This necessitates careful design of the experiment with appropriate controls. Due to a bias toward highly abundant proteins and potential co-purification of other proteins with probe targets, the negative controls of a proteomics experiment often do not cover the whole spectrum of background proteins. To combat this problem, twelve laboratories have combined the datasets of >300 negative control experiments to establish a database of common background proteins. This contaminant repository for affinity purification (CRAPome) is a useful database to identify common background proteins.[46] In case of affinity-based protein profiling, one also needs to keep in mind the specific background labeling proteins associated with each individual photoreactive group, which were mapped by Sieber and co-workers.[47] These datasets can be used to triage probe hits, but they are limited to background proteins based on the purification method[46] or photoreactive group.[47] When conducting chemical proteomics with lipid probes, one also has to account for the nonspecific interactions due to the inherent lipophilic character of these probes. A different set of background proteins could therefore be envisioned based on hydrophobic interactions with lipid probes.

To compile a database of promiscuous lipid-binding proteins, the reported enriched proteins from representative probes **8**, **14**, **15**, **19**, **21**, **22**, **23**, **27**, **29**, **33**, **40** and **47** were combined, compared and ranked. For each probe, the criteria of the authors for assigning probe targets were used. Where possible, the proteins identified in multiple cell lines were used. This resulted in a list of 1367 distinct proteins of which 176 targets were found in ≥4 experiments (from a total of 11 experiments) (Figure 10A). Of note, only 13 of these proteins were identified as background proteins by the CRAPome (using ≥20% of total entries as cut-off criteria).[46] An overview of the 176 promiscuous lipid-binding proteins can be found in the supplementary information (Table S1). It was found that photoaffinity probes **8**, **19** and **21** were highly selective with the smallest number of common targets (Figure 10B). For probe **8**, this was likely due its dissimilarity to the other probes with a highly negative charge at physiological pH. On the other hand, the caging groups of probes **19** and **21** seem to be effective for the reduction of non-specific labeling. All other probes had significant overlap of protein targets, and without diligent controls caution would be advised before calling these targets specific interaction partners.

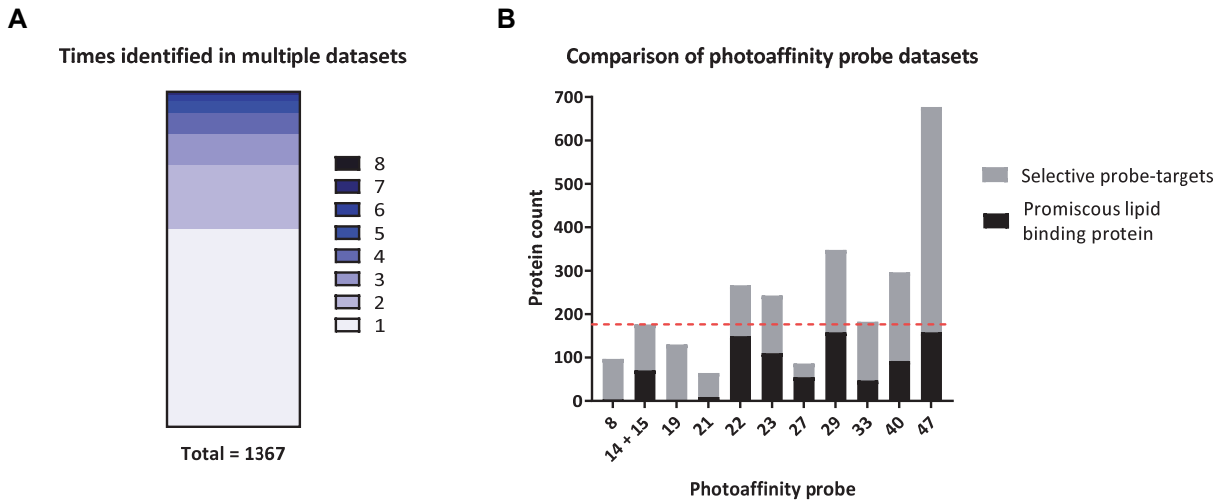

Figure 10 | Promiscuous lipid binder analysis. (A) Bar graph giving an overview of the amount of times proteins were identified in multiple datasets. In total 1367 proteins were identified of which 176 (13%) were found in at least 4 of the 11 datasets. A list is provided in Table S1. **(B)** Overview of the amount of probe-targets and promiscuous lipid binding proteins identified by each probe. The red line at 176 visualizes the maximum amount of promiscuous lipid binding proteins.

Conclusion

In summary, the aim of this chapter was to review the lipid-based photoaffinity probes published in the last decade. These probes constituted mainly of glycerol(phospho)lipid-, fatty acid-, sphingolipid- or sterol-based structures. Since the early development of lipid probes, the reported compounds have gained functionality while more closely resembling the structure of their parent lipids. Early probes usually contained benzophenones as reactive handles and a fluorescent or radiolabeled detection tag, which limited their application. Usually, binding to a known protein interaction partner was investigated. Benzophenones and aryl azides have made way for the diazirine moiety, due to the higher reactivity and smaller structural impact of this photoreactive group. The various detection tags on lipid probes have been replaced by an alkyne, which is minimally intrusive while being able to react with a large range of azide reagents. With improved synthetic and commercial access to photoreactive tools, lipid probes are now being used to map global lipid-protein interactions. Increasingly complex biological questions are being addressed, including lipid uptake, metabolism and localization.

There are number of caveats, however, to take into account when using lipid-based photoaffinity probes. For example, non-specific binding proteins, such as membrane-associated and internal membrane-bound proteins, are overrepresented as probe targets. Specific interaction partners might, therefore, be hard to identify. To combat this problem, appropriate controls should be included in the design of the experiment. Conventional competition experiments with an excess of non-probe competitor may give confounding results due to high lipophilicity and membrane accumulation of the competitor lipids.[48] It is, therefore, recommended to include structurally similar, but biologically inactive, probes to obtain a list of specific targets, which should be compared to lists of commonly found targets.[1,46,47] Another challenge is the fast metabolism of exogenous lipids, making it difficult to identify the biologically active lipid species. The addition of a caging group has been a successful strategy to allow for indiscriminate distribution of the probe before activation.[20,49] Lipid metabolism can also be exploited by incorporating the photoreactive and bioorthogonal handle into different lipid species, which results in the formation of a probe molecule *in situ*.[16]

Overall, lipid-based photoaffinity probes are useful chemical tools to study multiple aspects of lipid biology, using different techniques and compatible click reagents. Further development of these tools and their applications will allow for a more complete understanding of the many roles lipids play.

References

(1) Koenders, S. T. A.; Gagestein, B.; van der Stelt, M. Opportunities for Lipid-Based Probes in the Field of Immunology. In *Activity-Based Protein Profiling*; Cravatt, B. F., Hsu, K.-L., Weerapana, E., Eds.; Current Topics in Microbiology and Immunology; Springer International Publishing: Cham, 2019; pp 283–319.

(2) Haberkant, P.; Raijmakers, R.; Wildwater, M.; Sachsenheimer, T.; Brügger, B.; Maeda, K.; Houweling, M.; Gavin, A. C.; Schultz, C.; Van Meer, G.; Heck, A. J. R.; Holthuis, J. C. M. In Vivo Profiling and Visualization of Cellular Protein-Lipid Interactions Using Bifunctional Fatty Acids. *Angew. Chem. - Int. Ed.* **2013**, *52* (14), 4033–4038.

(3) Bush, J. T.; Walport, L. J.; McGouran, J. F.; Leung, I. K. H.; Berridge, G.; van Berkel, S. S.; Basak, A.; Kessler, B. M.; Schofield, C. J. The Ugi Four-Component Reaction Enables Expedient Synthesis and Comparison of Photoaffinity Probes. *Chem. Sci.* **2013**, *4* (11), 4115.

(4) Sakurai, K.; Ozawa, S.; Yamada, R.; Yasui, T.; Mizuno, S. Comparison of the Reactivity of Carbohydrate Photoaffinity Probes with Different Photoreactive Groups. *ChemBioChem* **2014**, *15* (10), 1399–1403.

(5) Dormán, G.; Prestwich, G. D. Benzophenone Photophores in Biochemistry. *Biochemistry* **1994**, *33* (19), 5661–5673.

(6) Buchmueller, K. L.; Hill, B. T.; Platz, M. S.; Weeks, K. M. RNA-Tethered Phenyl Azide Photocrosslinking via a Short-Lived Indiscriminant Electrophile. *J. Am. Chem. Soc.* **2003**, *125* (36), 10850–10861.

(7) Modarelli, D. A.; Morgan, S.; Platz, M. S. Carbene Formation, Hydrogen Migration, and Fluorescence in the Excited States of Dialkyldiazirines. *J. Am. Chem. Soc.* **1992**, *114* (18), 7034–7041.

(8) Ford, F.; Yuzawa, T.; Platz, M. S.; Matzinger, S.; Fülscher, M. Rearrangement of Dimethylcarbene to Propene: Study by Laser Flash Photolysis and Ab Initio Molecular Orbital Theory. *J. Am. Chem. Soc.* **1998**, *120* (18), 4430–4438.

(9) Yeagle, P. L. *The Membranes of Cells*; Academic Press, 2016.

(10) Bandyopadhyay, S.; Bong, D. Synthesis of Trifunctional Phosphatidylserine Probes for Identification of Lipid-Binding Proteins. *Eur. J. Org. Chem.* **2011**, No. 4, 751–758.

(11) Gubbens, J.; Ruijter, E.; de Fays, L. E. V.; Damen, J. M. A.; de Kruijff, B.; Slijper, M.; Rijkers, D. T. S.; Liskamp, R. M. J.; de Kroon, A. I. P. M. Photocrosslinking and Click Chemistry Enable the Specific Detection of Proteins Interacting with Phospholipids at the Membrane Interface. *Chem. Biol.* **2009**, *16* (1), 3–14.

(12) Rowland, M. M.; Bostic, H. E.; Gong, D.; Speers, A. E.; Lucas, N.; Cho, W.; Cravatt, B. F.; Best, M. D. Phosphatidylinositol 3,4,5-Trisphosphate Activity Probes for the Labeling and Proteomic Characterization of Protein Binding Partners. *Biochemistry* **2011**, *50* (51), 11143–11161.

(13) Gu, X.; Huang, Y.; Levison, B. S.; Gerstenecker, G.; DiDonato, A. J.; Hazen, L. B.; Lee, J.; Gogonea, V.; DiDonato, J. A.; Hazen, S. L. Identification of Critical Paraoxonase 1 Residues Involved in High Density Lipoprotein Interaction. *J. Biol. Chem.* **2016**, *291* (4), 1890–1904.

(14) Abe, M.; Nakano, M.; Kosaka, A.; Miyoshi, H. Syntheses of Photoreactive Cardiolipins for a Photoaffinity Labeling Study. *Tetrahedron Lett.* **2015**, *56* (17), 2258–2261.

(15) Peng, T.; Yuan, X.; Hang, H. C. Turning the Spotlight on Protein-Lipid Interactions in Cells. *Curr. Opin. Chem. Biol.* **2014**, *21*, 144–153.

(16) Wang, D.; Du, S.; Cazenave-Gassiot, A.; Ge, J.; Lee, J. S.; Wenk, M. R.; Yao, S. Q. Global Mapping of Protein–Lipid Interactions by Using Modified Choline-Containing Phospholipids Metabolically Synthesized in Live Cells. *Angew. Chem. - Int. Ed.* **2017**, *56* (21), 5829–5833.

(17) Ulivi, V.; Lenti, M.; Gentili, C.; Marcolongo, G.; Cancedda, R.; Descalzi Cancedda, F. Anti-Inflammatory Activity of Monogalactosyldiacylglycerol in Human Articular Cartilage in Vitro: Activation of an Anti-Inflammatory Cyclooxygenase-2 (COX-2) Pathway. *Arthritis Res. Ther.* **2011**, *13* (3), R92.

(18) Li, Z.; Hao, P.; Li, L.; Tan, C. Y. J.; Cheng, X.; Chen, G. Y. J.; Sze, S. K.; Shen, H.-M.; Yao, S. Q. Design and Synthesis of Minimalist Terminal Alkyne-Containing Diazirine Photo-Crosslinkers and Their Incorporation into Kinase Inhibitors for Cell- and Tissue-Based Proteome Profiling. *Angew. Chem. Int. Ed.* **2013**, *52* (33), 8551–8556.

(19) Liu, X.; Dong, T.; Zhou, Y.; Huang, N.; Lei, X. Exploring the Binding Proteins of Glycolipids with Bifunctional Chemical Probes. *Angew. Chem. - Int. Ed.* **2016**, *55* (46), 14330–14334.

(20) Höglinger, D.; Nadler, A.; Haberkant, P.; Kirkpatrick, J.; Schifferer, M.; Stein, F.; Hauke, S.; Porter, F. D.; Schultz, C. Trifunctional Lipid Probes for Comprehensive Studies of Single Lipid Species in Living Cells. *Proc. Natl. Acad. Sci.* **2017**, *114* (7), 1566–1571.

(21) Nadler, A.; Reither, G.; Feng, S.; Stein, F.; Reither, S.; Müller, R.; Schultz, C. The Fatty Acid Composition of Diacylglycerols Determines Local Signaling Patterns. *Angew. Chem. Int. Ed.* **2013**, *52* (24), 6330–6334.

(22) Spector, A. A.; Fang, X.; Snyder, G. D.; Weintraub, N. L. Epoxyeicosatrienoic Acids (EETs): Metabolism and Biochemical Function. *Prog. Lipid Res.* **2004**, *43* (1), 55–90.

(23) Chen, Y.; Falck, J. R.; Manthati, V. L.; Jat, J. L.; Campbell, W. B. 20-Iodo-14,15-Epoxyeicosa-8(Z)-Enoyl-3-Azidophenylsulfonamide: Photoaffinity Labeling of a 14,15-Epoxyeicosatrienoic Acid Receptor. *Biochemistry* **2011**, *50* (18), 3840–3848.

(24) Lee, K. S. S.; Henriksen, N. M.; Ng, C. J.; Yang, J.; Jia, W.; Morisseau, C.; Andaya, A.; Gilson, M. K.; Hammock, B. D. Probing the Orientation of Inhibitor and Epoxy-Eicosatrienoic Acid Binding in the Active Site of Soluble Epoxide Hydrolase. *Arch. Biochem. Biophys.* **2017**, *613*, 1–11.
(25) Peng, T.; Hang, H. C. Bifunctional Fatty Acid Chemical Reporter for Analyzing S-Palmitoylated Membrane Protein-Protein Interactions in Mammalian Cells. *J. Am. Chem. Soc.* **2015**, *137* (2), 556–559.
(26) Niphakis, M. J.; Lum, K. M.; Cognetta, A. B.; Correia, B. E.; Ichu, T. A.; Olucha, J.; Brown, S. J.; Kundu, S.; Piscitelli, F.; Rosen, H.; Cravatt, B. F. A Global Map of Lipid-Binding Proteins and Their Ligandability in Cells. *Cell* **2015**, *161* (7), 1668–1680.
(27) Lum, K. M.; Sato, Y.; Beyer, B. A.; Plaisted, W. C.; Anglin, J. L.; Lairson, L. L.; Cravatt, B. F. Mapping Protein Targets of Bioactive Small Molecules Using Lipid-Based Chemical Proteomics. *ACS Chem. Biol.* **2017**, *12* (10), 2671–2681.
(28) Haberkant, P.; Schmitt, O.; Contreras, F.-X.; Thiele, C.; Hanada, K.; Sprong, H.; Reinhard, C.; Wieland, F. T.; Brügger, B. Protein-Sphingolipid Interactions within Cellular Membranes. *J. Lipid Res.* **2008**, *49* (1), 251–262.
(29) Aureli, M.; Prioni, S.; Mauri, L.; Loberto, N.; Casellato, R.; Ciampa, M. G.; Chigorno, V.; Prinetti, A.; Sonnino, S. Photoactivable Sphingosine as a Tool to Study Membrane Microenvironments in Cultured Cells. *J. Lipid Res.* **2010**, *51* (4), 798–808.
(30) Haberkant, P.; Stein, F.; Höglinger, D.; Gerl, M. J.; Brügger, B.; Van Veldhoven, P. P.; Krijgsveld, J.; Gavin, A. C.; Schultz, C. Bifunctional Sphingosine for Cell-Based Analysis of Protein-Sphingolipid Interactions. *ACS Chem. Biol.* **2016**, *11* (1), 222–230.
(31) Hammerschmidt, P.; Ostkotte, D.; Nolte, H.; Gerl, M. J.; Jais, A.; Brunner, H. L.; Sprenger, H.-G.; Awazawa, M.; Nicholls, H. T.; Turpin-Nolan, S. M.; Langer, T.; Krüger, M.; Brügger, B.; Brüning, J. C. CerS6-Derived Sphingolipids Interact with Mff and Promote Mitochondrial Fragmentation in Obesity. *Cell* **2019**, *177* (6), 1536-1552.e23.
(32) Deng, Y.; Pakdel, M.; Blank, B.; Sundberg, E. L.; Burd, C. G.; von Blume, J. Activity of the SPCA1 Calcium Pump Couples Sphingomyelin Synthesis to Sorting of Secretory Proteins in the Trans-Golgi Network. *Dev. Cell* **2018**, *47* (4), 464-478.e8.
(33) Bockelmann, S.; Mina, J. G. M.; Korneev, S.; Hassan, D. G.; Müller, D.; Hilderink, A.; Vlieg, H. C.; Raijmakers, R.; Heck, A. J. R.; Haberkant, P.; Holthuis, J. C. M. A Search for Ceramide Binding Proteins Using Bifunctional Lipid Analogs Yields CERT-Related Protein StarD7. *J. Lipid Res.* **2018**, *59* (3), 515–530.
(34) Dadsena, S.; Bockelmann, S.; Mina, J. G. M.; Hassan, D. G.; Korneev, S.; Razzera, G.; Jahn, H.; Niekamp, P.; Müller, D.; Schneider, M.; Tafesse, F. G.; Marrink, S. J.; Melo, M. N.; Holthuis, J. C. M. Ceramides Bind VDAC2 to Trigger Mitochondrial Apoptosis. *Nat. Commun.* **2019**, *10* (1), 1–12.
(35) Jiang, X.; Zhu, Z.; Qin, H.; Tripathi, P.; Zhong, L.; Elsherbini, A.; Karki, S.; Crivelli, S. M.; Zhi, W.; Wang, G.; Spassieva, S. D.; Bieberich, E. Visualization of Ceramide-Associated Proteins in Ceramide-Rich Platforms Using a Cross-Linkable Ceramide Analog and Proximity Ligation Assays With Anti-Ceramide Antibody. *Front. Cell Dev. Biol.* **2019**, *7*.
(36) Kong, J.-N.; Zhu, Z.; Itokazu, Y.; Wang, G.; Dinkins, M. B.; Zhong, L.; Lin, H.-P.; Elsherbini, A.; Leanhart, S.; Jiang, X.; Qin, H.; Zhi, W.; Spassieva, S. D.; Bieberich, E. Novel Function of Ceramide for Regulation of Mitochondrial ATP Release in Astrocytes. *J. Lipid Res.* **2018**, *59* (3), 488–506.
(37) Pike, L. J. Lipid Rafts. *J. Lipid Res.* **2003**, *44* (4), 655–667.
(38) Hulce, J. J.; Cognetta, A. B.; Niphakis, M. J.; Tully, S. E.; Cravatt, B. F. Proteome-Wide Mapping of Cholesterol-Interacting Proteins in Mammalian Cells. *Nat. Methods* **2013**, *10* (3), 259–264.
(39) Budelier, M. M.; Cheng, W. W. L.; Bergdoll, L.; Chen, Z. W.; Janetka, J. W.; Abramson, J.; Krishnan, K.; Mydock-McGrane, L.; Covey, D. F.; Whitelegge, J. P.; Evers, A. S. Photoaffinity Labeling with Cholesterol Analogues Precisely Maps a Cholesterol-Binding Site in Voltage-Dependent Anion Channel-1. *J. Biol. Chem.* **2017**, *292* (22), 9294–9304.
(40) Byrd, K. M.; Arieno, M. D.; Kennelly, M. E.; Estiu, G.; Wiest, O.; Helquist, P. Design and Synthesis of a Crosslinker for Studying Intracellular Steroid Trafficking Pathways. *Bioorg. Med. Chem.* **2015**, *23* (13), 3843–3851.
(41) Zhou, H.; Hylemon, P. B. Bile Acids Are Nutrient Signaling Hormones. *Steroids* **2014**, *86*, 62–68.
(42) Zhuang, S.; Li, Q.; Cai, L.; Wang, C.; Lei, X. Chemoproteomic Profiling of Bile Acid Interacting Proteins. *ACS Cent. Sci.* **2017**, *3* (5), 501–509.
(43) Guo, H.; Xu, J.; Hao, P.; Ding, K.; Li, Z. Competitive Affinity-Based Proteome Profiling and Imaging to Reveal Potential Cellular Targets of Betulinic Acid. *Chem. Commun.* **2017**, *53* (69), 9620–9623.
(44) Herner, A.; Marjanovic, J.; Lewandowski, T. M.; Marin, V.; Patterson, M.; Miesbauer, L.; Ready, D.; Williams, J.; Vasudevan, A.; Lin, Q. 2-Aryl-5-Carboxytetrazole as a New Photoaffinity Label for Drug Target Identification. *J. Am. Chem. Soc.* **2016**, *138* (44), 14609–14615.
(45) Zhang, L.; Zhang, Y.; Dong, J.; Liu, J.; Zhang, L.; Sun, H. Design and Synthesis of Novel Photoaffinity Probes for Study of the Target Proteins of Oleanolic Acid. *Bioorg. Med. Chem. Lett.* **2012**, *22* (2), 1036–1039.
(46) Mellacheruvu, D.; Wright, Z.; Couzens, A. L.; Lambert, J. P.; St-Denis, N. A.; Li, T.; Miteva, Y. V; Hauri, S.; Sardiu, M. E.; Low, T. Y.; Halim, V. A.; Bagshaw, R. D.; Hubner, N. C.; Al-Hakim, A.; Bouchard, A.; Faubert, D.; Fermin, D.; Dunham, W. H.; Goudreault, M.; Lin, Z. Y.; Badillo, B. G.; Pawson, T.; Durocher, D.;

Coulombe, B.; Aebersold, R.; Superti-Furga, G.; Colinge, J.; Heck, A. J. R.; Choi, H.; Gstaiger, M.; Mohammed, S.; Cristea, I. M.; Bennett, K. L.; Washburn, M. P.; Raught, B.; Ewing, R. M.; Gingras, A. C.; Nesvizhskii, A. I. The CRAPome: A Contaminant Repository for Affinity Purification-Mass Spectrometry Data. *Nat. Methods* **2013**, *10* (8), 730–736.

(47) Kleiner, P.; Heydenreuter, W.; Stahl, M.; Korotkov, V. S.; Sieber, S. A. A Whole Proteome Inventory of Background Photocrosslinker Binding. *Angew. Chem. - Int. Ed.* **2017**, *56* (5), 1396–1401.

(48) Mbarik, M.; Biam, R. S.; Robichaud, P.-P.; Surette, M. E. The Impact of PUFA on Cell Responses: Caution Should Be Exercised When Selecting PUFA Concentrations in Cell Culture. *Prostaglandins Leukot. Essent. Fatty Acids* **2020**, 102083.

(49) Laguerre, A.; Hauke, S.; Qiu, J.; Kelly, M. J.; Schultz, C. Photorelease of 2-Arachidonoylglycerol in Live Cells. *J. Am. Chem. Soc.* **2019**, *141* (42), 16544–16547.

Supplementary data

Table S1 | List of proteins identified as promiscuous lipid binding proteins. Proteins are listed with their accession number, gene name and the number of datasets in which they were identified as a probe target. Proteins colored red are the proteins flagged by the CRAPome database.

Accession number	Gene name	Count	Accession number	Gene name	Count	Accession number	Gene name	Count	Accession number	Gene name	Count
Q9NRG9	AAAS	4	A0FGR8	ESYT2	4	Q9Y5Y5	PEX16	5	P43307	SSR1	8
P28288	ABCD3	5	Q9NRY5	FAM114A2	7	O00264	PGRMC1	7	P51571	SSR4	6
O95870	ABHD16A	4	Q96A26	FAM162A	4	O15173	PGRMC2	6	Q9NQZ5	STARD7	4
Q8WTS1	ABHD5	4	Q8WVX9	FAR1	4	P35232	PHB	6	Q9UJZ1	STOML2	4
Q9BV23	ABHD6	7	P37268	FDFT1	4	Q99623	PHB2	7	P46977	STT3A	4
O95573	ACSL3	4	P22830	FECH	4	Q92643	PIGK	5	Q8TCJ2	STT3B	4
Q9BRR6	ADPGK	5	O00461	GOLIM4	5	Q96S52	PIGS	5	Q9UH99	SUN2	4
O95831	AIFM1	5	Q9P035	HACD3	4	Q9H490	PIGU	4	O15260	SURF4	5
P51648	ALDH3A2	7	P40939	HADHA	6	Q10713	PMPCA	4	Q9Y4P3	TBL2	6
P53365	ARFIP2	6	Q9NRV9	HEBP1	4	P50897	PPT1	5	Q9NZ01	TECR	4
Q8NHH9	ATL2	4	Q8TCT9	HM13	6	Q9BZL6	PRKD2	4	P0DO92	T-ENOL	4
Q6DD88	ATL3	4	P30519	HMOX2	6	Q9H7Z7	PTGES2	4	Q8WUY1	THEM6	4
Q9HD20	ATP13A1	6	Q53GQ0	HSD17B12	6	P18031	PTPN1	4	O60830	TIMM17B	4
P16615	ATP2A2	6	Q3SXM5	HSDL1	5	P61026	RAB10	5	O14925	TIMM23	5
P25705	ATP5A1	4	P14625	HSP90B1	4	P62491	RAB11A	4	O43615	TIMM44	5
P06576	ATP5B	4	P11021	HSPA5	4	P62820	RAB1A	4	Q3ZCQ8	TIMM50	5
P24539	ATP5F1	5	O60725	ICMT	4	Q9H0U4	RAB1B	4	Q13445	TMED1	4
Q93050	ATP6V0A1	4	Q8TCB0	IFI44	4	Q8TC12	RDH11	4	P49755	TMED10	5
Q9UHQ4	BCAP29	4	Q70UQ0	IKBIP	4	P04843	RPN1	6	Q15363	TMED2	5
P51572	BCAP31	7	Q16891	IMMT	4	P04844	RPN2	5	Q9Y3B3	TMED7	4
Q8WY22	BRI3BP	5	Q8N5M9	JAGN1	4	O95197	RTN3	5	Q9NX00	TMEM160	5
P35613	BSG	4	P24390	KDELR1	4	Q9NQC3	RTN4	5	Q9HC07	TMEM165	4
P27824	CANX	6	Q06136	KDSR	5	Q9NTJ5	SACM1L	4	Q6NUQ4	TMEM214	5
Q96A33	CCDC47	8	Q86SY8	KTN1-AS1	5	Q9Y512	SAMM50	7	Q4ZIN3	TMEM259	4
Q96G23	CERS2	6	Q14739	LBR	4	Q9NR31	SAR1A	4	P57088	TMEM33	5
Q9NZ45	CISD1	6	O95202	LETM1	5	Q9Y6B6	SAR1B	4	Q9BTV4	TMEM43	5
Q07065	CKAP4	6	P20700	LMNB1	4	Q8WTV0	SCARB1	4	P42166	TMPO	6
Q9UBD9	CLCF1	4	Q6P1A2	LPCAT3	4	Q14108	SCARB2	4	Q9H3N1	TMX1	5
O96005	CLPTM1	6	Q96AG4	LRRC59	7	Q8NBX0	SCCPDH	5	Q9Y320	TMX2	5
P23786	CPT2	5	Q9NZJ7	MTCH1	5	O43819	SCO2	4	Q9NS69	TOMM22	5
P07339	CTSD	5	Q9Y6C9	MTCH2	6	P67812	SEC11A	4	O96008	TOMM40	4
Q6UW02	CYP20A1	4	Q86UE4	MTDH	7	Q9UGP8	SEC63	4	O14656	TOR1A	5
Q16850	CYP51A1	7	Q969V3	NCLN	5	Q9UBV2	SEL1L	7	Q9H4I3	TRABD	4
Q8WVC6	DCAKD	5	Q9Y6Q9	NCOA3	6	Q8IWL2	SFTPA1	5	O95292	VAPB	4
O15121	DEGS1	4	Q9BTX1	NDC1	4	O95470	SGPL1	5	P21796	VDAC1	6
Q9BUN8	DERL1	5	Q9Y639	NPTN	4	P53007	SLC25A1	4	P45880	VDAC2	5
Q15392	DHCR24	6	Q15738	NSDHL	5	Q9UBX3	SLC25A10	5	P08670	VIM	4
Q96LJ7	DHRS1	5	Q02818	NUCB1	5	Q02978	SLC25A11	4	Q8N0U8	VKORC1L1	6
Q9Y394	DHRS7	5	P80303	NUCB2	4	O75746	SLC25A12	5	Q96GC9	VMP1	4
Q96KC8	DNAJC1	4	Q8TEM1	NUP210	4	O43772	SLC25A20	4	Q5BJH7	YIF1B	4
Q8N766	EMC1	4	Q8NFH5	NUP35	4	Q9H2D1	SLC25A32	4	O75844	ZMPSTE24	7
P50402	EMD	7	Q9NX40	OCIAD1	6	P05141	SLC25A5	4			
P07099	EPHX1	5	O60313	OPA1	4	Q8TAD4	SLC30A5	4			
O75477	ERLIN1	5	P07237	P4HB	4	Q15005	SPCS2	4			
Q9BSJ8	ESYT1	4	Q9UHG3	PCYOX1	6	Q14534	SQLE	4			